JOURNAL OF MATERIALS SCIENCE 27 (1992) 5281–5285

Reversible structural relaxation of amorphous $Ni_{70}TM_5Si_{10}B_{15}$ (TM=V, Cr, Mn, Fe, Co, Ni) alloys

O. HARUYAMA, N. ASAHI
Department of Physics, Faculty of Science and Technology, Science University of Tokyo, 2641 Yamazaki, Noda, Chiba, 278 Japan

The structural relaxation of amorphous $Ni_{70}TM_5Si_{10}B_{15}$ (TM = V, Cr, Mn, Fe, Co, Ni) alloy was investigated by the electrical resistance measurement under isochronal annealing. The reference $Ni_{75}Si_{10}B_{15}$ alloy showed no reversible changes in electrical resistance. All alloys other than TM = Ni exhibited a reversible change which is peculiar to the chemical short-range ordering. Only in TM = Cr alloy was the reversible part predominantly observed after pre-annealing, and in other alloys the irreversible change was also seen. The degree of reversible change below 623 K was in the order Fe > V > Cr > Co > Mn. This origin is discussed on the basis of Ni–TM correlation, which is considered to play an important role in ordering, and TM–metalloid correlation, which is considered to hinder the formation of an ordered phase.

1. Introduction

An amorphous phase is thermodynamically in a non-equilibrium state and transforms into a crystalline phase on thermal treatments. Below the crystallization temperature, the structural relaxation is also known to occur. The structural relaxation is generally classified into two types [1–3]: topological short-range ordering (TSRO), originating from atomic movements accompanied by the annihilation of density fluctuation during heat treatments, and chemical short-range ordering (CSRO). Although CSRO is qualitatively considered to occur by atomic rearrangements during annealing [1], the universal model to explain CSRO does not seem to be proposed. However, it has been suggested that CSRO is importantly related to the correlation between constituent metals in several alloy systems [1–3]. Therefore, it is necessary to study the CSRO behaviour for various alloy systems as well as their mechanisms. In nickel-based amorphous alloys, the addition of titanium [1], chromium [4], iron [5, 6], zirconium [7] and palladium [8] to the nickel matrix has been reported to induce CSRO. However, there are a few papers which systematically compare the CSRO behaviour in amorphous Ni–TM–metalloid alloys. Drittler *et al.* [9] have recently calculated the solution energy of 3d transition impurity in a nickel crystal, and showed that their results are qualitatively coincident with the experimental ones. It is well known that the solution energy is closely related to the binding energy of the atoms and this motivated the present work, in which we studied the structural relaxation in amorphous $Ni_{70}TM_5Si_{10}B_{15}$ (TM = V, Cr, Mn, Fe, Co, Ni) alloy. A mutual comparison of CSRO behaviour observed in the alloys, except TM = Ni, is reported, and the difference in the strength between Ni–TM and metal–metalloid correlations are discussed to explain the relaxation behaviour in each alloy.

2. Experimental procedure

The amorphous ribbons with composition $Ni_{70}TM_5Si_{10}B_{15}$ (TM = V, Cr, Mn, Fe, Co, Ni) were prepared by a melt-spinning method with a single copper roller in an argon atmosphere. They were about 20 μm thick and 2 mm wide. The X-ray diffraction patterns of ribbons showed no crystalline peaks. To study the crystallization behaviour of the sample, the differential scanning calorimeter (DSC) and electrical resistance measurements were carried out at a heating rate of $20\ \mathrm{K\,min^{-1}}$. The structural relaxation was studied by the change in electrical resistance at 77 K after an isochronal annealing of 10 min. The conventional d.c. technique was used in electrical resistance measurement. The isochronal annealing was accomplished using infrared image furnace in a helium atmosphere, when the intended annealing temperature was reached at a mean heating rate of $300\ \mathrm{K\,min^{-1}}$.

3. Results and discussion

Fig. 1 shows the DSC thermograms of each alloy to investigate thermal behaviour near crystallization, where the crystallization temperature T_x, was defined as a departure from the base line. To minimize the ambiguity of T_x, measurements were repeated three times and the mean value was adopted as T_x. The changes in electrical resistance, $\Delta R/R_{asq}$, with isochronal annealing from room temperature are shown in

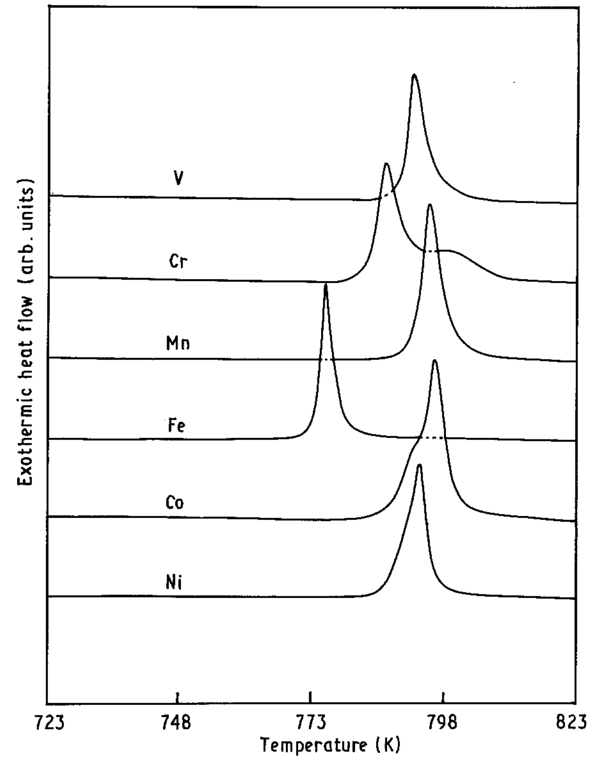

Figure 1 DSC thermograms for amorphous $Ni_{70}TM_5Si_{10}B_{15}$ alloys. Heating rate 20 K min^{-1}. The crystallization temperature, T_x, was defined as a departure from the base line.

Fig. 2a–f, where R_{asq} represents the resistance values at 77 K in an as-quenched state and ΔR is defined as R-R_{asq}. The figures show that the resistance value decreases with the development of crystallization for both TM = Ni and Co, and increases, on the contrary, in other alloys. It is necessary to carry out isochronal

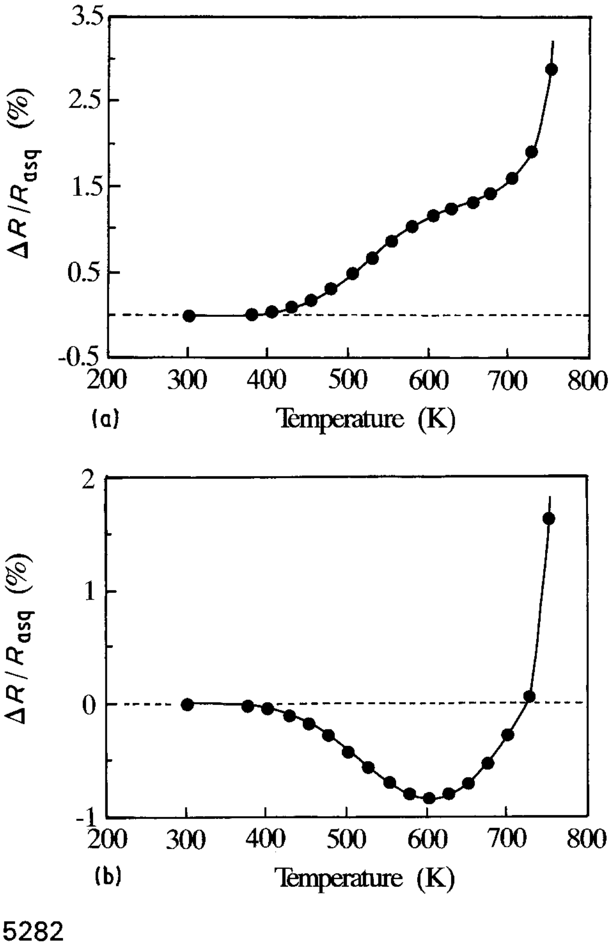

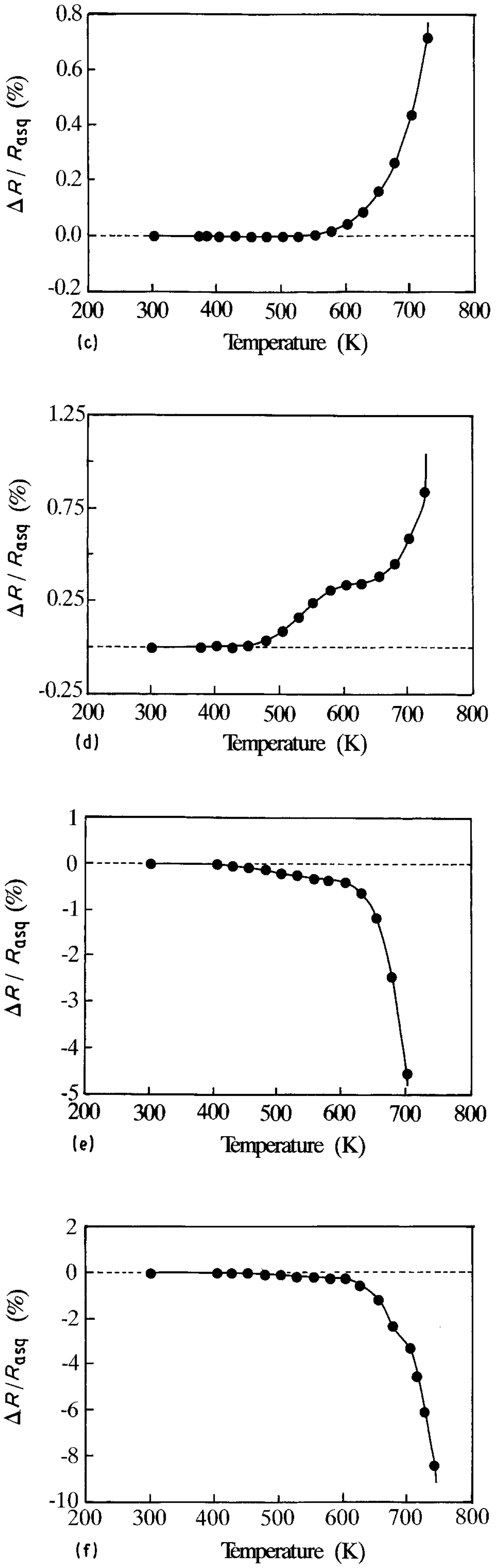

Figure 2 The changes in electrical resistance with isochronal annealing temperature for $Ni_{70}TM_5Si_{10}B_{15}$ alloys in an as-quenched state: TM = (a) V, (b) Cr, (c) Mn, (d) Fe, (e) Co and (f) Ni.

annealing in a relative low temperature region to check whether or not CSRO takes place [1, 3]. However, the release of quenched-in stress and the annihilation of free volume (density fluctuation) occur simultaneously in a similar temperature region. Accordingly, the sample must be pre-annealed to minimize their effects and to identify CSRO [2, 3]. Taking account of T_x and Fig. 2, the pre-annealing temperature, T_p, was determined for each alloy to be about 100 K lower than T_x. Pre-annealing times, t_p, from 30–50 min were used in this experiment. T_x, T_p and t_p are summarized in Table I.

TABLE I The crystallization temperature, T_x, pre-annealing temperature, T_p, and time, t_p, and the total reversible change, β, of resistance due to the formation of CSRO.

	V	Cr	Mn	Fe	Co	Ni
T_x (K)	781	775	783	769	778	777
T_p (K)	674	668	663	674	673	653
t_p (min)	30	50	30	50	30	30
β (%)	0.06	− 0.05	0.005	0.12	− 0.025	0

Fig. 3a–f show the changes in electrical resistance, $\Delta R/R_p$, with isochronal annealing for pre-annealed samples, where R_p represents the resistance value at 77 K just after pre-annealing. Here, the first curve was taken in a cooling mode and the second was measured in a heating mode, and these modes were repeated in subsequent annealing cycles. For TM = Ni, Fig. 3f, the resistance decreases with the repetition of annealing cycle. That is, the reversible part of resistance

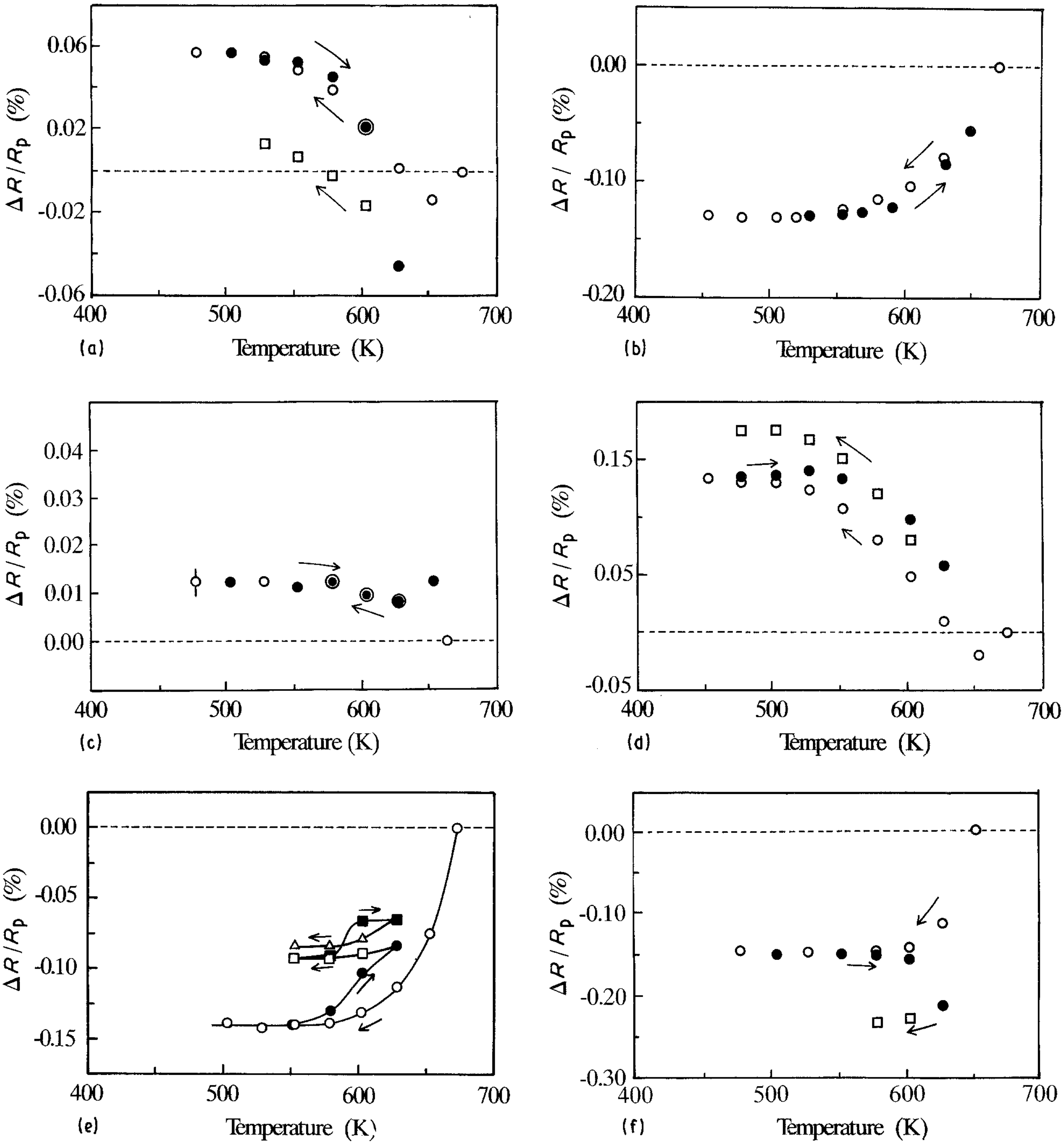

Figure 3 The changes in electrical resistance during isochronal annealing cycles for pre-annealed $Ni_{70}TM_5Si_{10}B_{15}$ alloys. TM = (a) V, (b) Cr, (c) Mn, (d) Fe, (e) Co and (f) Ni, where (○), (□) and (△) represent the first, second and third cooling runs, and (●) and (■) correspond to the first and second heating runs.

change, which is peculiar to the formation and decomposition process of an ordered phase, is not observed in the curves. It may be considered that the amorphous structure of this alloy was not stabilized by pre-annealing, so that the free volume continued to decrease during the annealing cycle. Balanzat *et al.* [1] reported that amorphous $Fe_{81.5}Si_4B_{14.5}$ and $Pd_{78}Ge_{22}$ alloys show a reversible change in isochronal measurements of electrical resistance. Takahara *et al.* [10] have also reported a similar reversible change in electrical resistance measurements by using amorphous $Fe_{78}Si_{15}B_7$ alloy, and attributed this phenomenon to Fe–Si correlation. Therefore, it is important that the amorphous $Ni_{75}Si_{10}B_{15}$ alloy does not show CSRO, because other alloys are prepared by the substitution of 5 at % TM for nickel and thus the reversible changes in resistance may be attributed to CSRO change resulting from Ni–TM correlation. All alloys other than TM = Ni show reversible changes during the isochronal annealing cycles. In the case of TM = Cr especially, Fig. 3b, the reversible change on the curves for runs 1 and 2 can be observed to predominate and the irreversible change becomes significantly small. However, alloys other than TM = Cr also show a shift in the curves, due to irreversible changes, which is considered to originate from the lack of stabilization of the sample during pre-annealing. To research and compare the behaviour of CSRO in these alloys, the total change, β, in electrical resistance due to the formation of an ordered phase was estimated using the second cooling curve (third run curve) within the temperature region below 623 K. β for each alloy is represented in Table I, where the plus and minus signs indicate that the electrical resistance increases and decreases, respectively, with the formation of an ordered phase. Furthermore, the absolute value, |β|, falls in the order Fe > V > Cr > Co > Mn. In many alloy systems, the metal–metal correlation has been reported to be important in understanding CSRO [1, 3]. As there are few reports concerning the strength of Ni–TM correlation in nickel-based amorphous alloys, we consider it in crystalline alloys instead. Drittler *et al.* [9] has estimated the solution energy, E_s, for the various 3d transition impurities substituted into crystalline nickel to perform a relative comparison of the Ni–TM correlation. Fig. 4 shows the results obtained by Drittler *et al.* [9] together with the experimental [11] and Miedema's semi-empirical results [12]. Following their suggestions, the larger minus value of E_s means a stronger correlation between nickel and the 3d element. Fig. 4 shows that $|E_s|$ is qualitatively in the order V > Mn > Fe > Cr > Co. This result is, however, not in accordance with the order of |β| mentioned above. So it is impossible to explain the order of |β| merely from Ni–TM correlation. It should be noticed that the 3d element substituted produces a new bonding with metalloid atoms, boron and silicon in this case. Consider T_x as a measure of bonding strength between metal and metalloid atoms, because the stronger covalence between metal and metalloid atoms should result in a higher crystallization temperature in order to suppress atomic movements. Then the bonding strength with metalloid atoms may be said to give the order Mn > V > Co (≈ Ni) > Cr > Fe, at least as long as $Ni_{70}TM_5Si_{10}B_{15}$ alloys are concerned. By comparing the order of T_x and $|E_s|$ mentioned above, it may be reasonable to presume that the higher T_x suppresses the appearance of CSRO, and the larger $|E_s|$, on the contrary, promotes CSRO. That is, the TM = Mn alloy has the second largest $|E_s|$ of all the alloys, but |β| is the least. It may be considered that the formation of the nickel and manganese atom pairs is suppressed by the strong bonding between the manganese and metalloid atoms. Although the TM = Fe alloy has a relatively small $|E_s|$, |β| takes a much larger value. In this alloy, the formation of nickel and iron atom pairs may be enhanced by the weaker bonding between ion and metalloid atoms than that between nickel and metalloid atoms. The TM = V alloy has the largest value of $|E_s|$. However, this alloy system also has a relatively high value of T_x. The competition between these two effects presumably decides |β| in this alloy. Although the TM = Cr alloy has a relatively small value of $|E_s|$, the reversible change in electrical resistance clearly appears. This may be attributed to the much smaller T_x (next to TM = Fe alloy). The TM = Co alloy has a similar value of T_x to TM = Ni alloy and $|E_s|$ has the smallest value of all alloy systems, so that |β| may have a much smaller value.

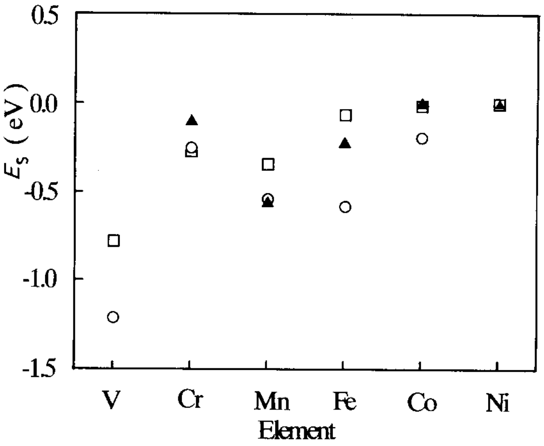

Figure 4 The solution energy of a 3d element substituted into crystalline nickel: (○) Drittler [9], (□) Miedema [12], (▲) experiment [11].

The sign of β varies in alloy systems. This phenomenon has also been observed in other alloy systems [13]. Although there is so far no decisive explanation of it, the differrence in electrical transport properties in the alloy system may be suggestive. It has been reported [14] that the electrical transport properties of amorphous Ni–Si–B alloys changed significantly on the addition of 3d elements. In amorphous $Ni_{70}TM_5Si_{10}B_{15}$ alloys, a similar phenomenon may be expected to occur. Fig. 5 shows the temperature coefficient of resistance (TCR) at room temperature for as-quenched and pre-annealed samples. The TCR was estimated from resistance data measured in the temperature region from room temperature to 373 K at a heating rate of $2\,K\,min^{-1}$. The TCR for as-quenched samples has a positive value in alloys other

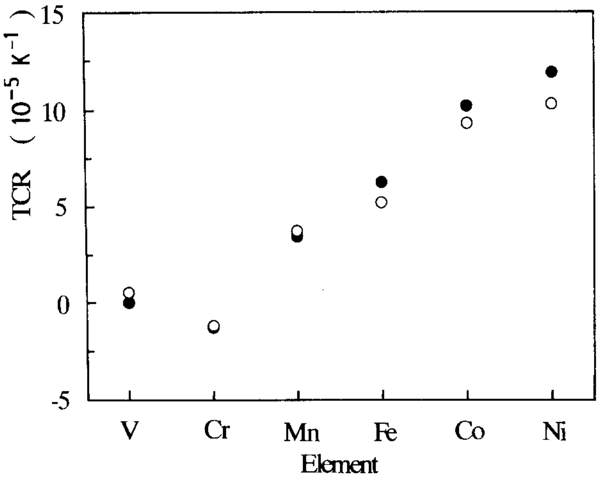

Figure 5 The temperature coefficient of resistance, TCR, at room temperature for (○) as-quenched and (●) pre-annealed $Ni_{70}TM_5Si_{10}B_{15}$ alloys: TM = V, Cr, Mn, Fe, Co and Ni.

than TM = Cr. This agrees with the results reported by Park and Sostarich [14]. After pre-annealing, the behaviour of TCR is classified into two groups: one group, to which TM = Fe, Co and Ni belong, represents a smaller value of TCR than that for an as-quenched sample; the other group shows, on the contrary, a larger TCR than that for the as-quenched sample. This may suggest different electrical transport properties in the two groups. However, as the alloys in the same group show dissimilar signs of β, further measurements of electriccal transport properties will be required to elucidate the behaviour of β in amorphous $Ni_{70}TM_5Si_{10}B_{15}$ alloys.

4. Conclusion

The reversible relaxation in amorphous $Ni_{70}TM_5Si_{10}B_{15}$ (TM = V, Cr, Mn, Fe, Co, Ni) alloys was examined by electrical resistance measurements. Alloys other than TM = Ni showed a reversible change in electrical resistance during isochronal annealing. However, in alloys other than TM = Cr, an additional irreversible change was also observed. The reversible change was large, in the order Fe > V > Cr > Co > Mn. This origin was qualitatively interpreted by the competition of metal–metal and metal–metalloid correlations in alloy systems. The strength of metal–metal correlation was estimated [9] by considering the solution energy of crystalline nickel containing transition metal impurities. The metal–metalloid correlations were predicted from the crystallization temperature in the amorphous alloys.

References

1. E. BALANZAT, J. T. STANLEY, C. MAIRY and J. HILLAIRET, *Acta Metall.* **33** (1985) 785.
2. A. BEUKEL, S. ZWAAG and A. L. MULDER, *ibid.* **32** (1984) 1895.
3. T. KOMATSU, K. IWASAKI, S. SATO and K. MATUSITA, *J. Appl. Phys.* **64** (1988) 4853.
4. O. HARUYAMA and N. ASAHI, *J. Mater. Sci.* in press.
5. T. KOMATSU and K. MATUSITA, *ibid.* **21** (1986) 1693.
6. R. BRUNING, Z. ALTOUNIAN and J. O. STROM-OLSEN, *J. Appl. Phys.* **62** (1987) 3633.
7. J. HILLAIRET, E. BALANZAT, N. E. DERRADJI and A. CHAMBEROD, *J. Non-Cryst. Solids* **61, 62** (1984) 781.
8. J. D. COMINS, J. E. MACDONALD, M. R. J. GIBBS and G. A. SAUNDERS, *J. Phys. F Met. Phys.* **17** (1987) 19.
9. B. DRITTLER, M. WEINERT, R. ZELLER and P. H. DEDERICHS, *Phys. Rev. B* **39** (1989) 930.
10. Y. TAKAHARA, K. HATADE and H. MATSUDA, *Trans. JIM* **29** (1988) 774.
11. U. V. BARTH and L. HEDIN, *J. Phys. C* **5** (1972) 1629.
12. A. R. MIEDEMA, P. F. de CHATEL and F. R. de BOER, *Physica B* **100** (1980) 1.
13. T. KOMATSU, R. YOKOTA, T. SHINDO and K. MATUSITA, *J. Non-Cryst. Solids* **65** (1984) 63.
14. T. S. PARK and M. SOSTARICH, *J. Appl. Phys.* **53** (1982) 8251.

Received 11 June
and accepted 28 October 1991